Single-Ended Infrared Photothermal Radiometric Measurement of Quantum Efficiency and Metastable Lifetime in Solid-State Laser Materials: The Case of Ruby ($Cr^{3+}:Al_2O_3$)

Andreas Mandelis, Mahendra Munidasa, and Andreas Othonos

Abstract—**A new, simple, and self-consistent frequency-scanned photothermal radiometric (PTR) detection scheme was applied to the measurement of the metastable state de-excitation parameters of a ruby laser rod. From the extrema of the photothermal phase and the amplitude slope versus the excitation laser beam modulation frequency curves, we have calculated the radiative quantum efficiency and lifetime in this material, without recourse to the conventional second measurement to eliminate effects of photothermal saturation. This technique simplifies significantly the experimental methodology, guarantees uniqueness of the measured quantities, and increases the measurement range of lifetimes as compared to other photothermal-based methods. Therefore, it may prove valuable as a fast industrial quality control, as well as for fundamental studies of laser materials.**

I. Introduction

PHOTOACOUSTIC spectroscopy (PAS) was utilized early on in the study of nonradiative processes in luminescent systems exhibiting metastable excited-state structure [1], [2]. The advantage of this technique over purely optical methods is its ability to measure the *absolute* nonradiative quantum efficiency η_{NR}. This, in turn, can be readily used to determine the *absolute* radiative quantum efficiency, $\eta_R = 1 - \eta_{NR}$, without recourse to complicated and often inaccurate absolute detector calibration procedures such as the integrating sphere method, or knowledge of absolute ion concentrations in the case of solid-state laser media [3]. This important feature of PAS has been exploited by Murphy and Aamodt [4] in interpreting the observed concentration-dependent metastable level quenching rates in ruby. Other authors have also applied PAS to the study of luminescence quantum efficiencies of laser-type solids [5], [6] and liquids [7]. At the same time, the ability of PAS to yield measurements of metastable lifetimes in laser materials has been demonstrated, essentially independently from the quantum efficiency measurements [1], [8]. These measurements were spectroscopic and, as a rule, difficult to interpret.

Quimby and Yen [9] have developed a working photoacoustic technique to determine η_R in solid-state laser materials, which depends on the measurement of the PAS phase. This technique can, in principle, estimate *both* the quantum efficiency η_R and the metastable lifetime τ. Besides ruby, it has also been used successfully with alexandrite [10]. In practice, however, there are several disadvantages: in order to eliminate the effects of both PAS saturation (i.e., the often nonlinear signal frequency response dependence on the optical absorption coefficient of the material), two optical excitation wavelengths are required with (ideally) equal absorption coefficients. This can only be attained if, by coincidence, the available laser source can operate at two separate lines at which the sample exhibits nearly equal absorption coefficients, as is the case of ruby and the Krypton laser: the latter emits at 407 and 568 nm, for which lines the absorption coefficients β are nearly equal in $E \perp c$ polarization ($\beta \approx 41$ cm^{-1}, $\Delta\beta = 1.2$ cm^{-1}) [9]. A less accidental but more labor and instrumentation-intensive method is to adjust the polarization of the laser beam by rotation with respect to the c axis of the crystal [10], so that the absorption at the two operating lines may become nearly equal. Under these nearly ideal conditions, and assuming one-dimensional (1-D) PAS response, the PAS phase difference between the two signal at the two exciting wavelengths is a rather simple function of η_{NR} and τ, which yields these two parameters through the best fit of the theory to the data. This method, albeit very important as the simplest and most straightforward measurement technique of η_{NR} (and consequently η_R) to date, unfortunately, does not guarantee the uniqueness of the two-parameter (η_R, τ) fit. Besides, it is experimentally awkward and time consuming as it requires the aforementioned β adjustment, coupled with two sets of frequency measurements, one at each excita-

Manuscript received May 25, 1992; revised November 1, 1992.

The work was supported by a Strategic Grant from the Natural Sciences and Engineering Research Council of Canada (NSERC).

The authors are with the Photothermal and Optoelectronic Diagnostics Laboratory, and the Ontario Laser and Lightwave Research Center, Department of Mechanical Engineering, University, of Toronto, Toronto, Canada MSS 1A4.

IEEE Log Number 9209103.

tion wavelength. Most importantly, i) the required signal phase difference recording at each modulation frequency appears to produce significant scatter to the data, which compromises the measurement accuracy in an already low signal-to-noise ratio (SNR) situation, such as is the case with high-quality laser materials ($\eta_{NR} < 0.1$); and ii) PA detection is intrinsically severely limited to low-frequency measurements by the significant roll-off of the microphone transfer function [11]. This important drawback limits the acceptable SNR to a range of lifetimes of several hundred μs, at best. Ruby ($\tau \approx 2.7$ ms [9]) and alexandrite ($\tau = 260$ μs [10]) are but two of all the interesting and important laser materials with (usually) much shorter relaxation time constants. A case in point is the highly promising $Ti^{3+}:Al_2O_3$ crystal ($\tau = 3.3$ μs at $T = 300$ K [12]). It is necessary to be able to access modulation frequencies on the order of the inverse lifetime in order to obtain *both* η_{NR} and τ information.

In this paper we sought to eliminate the deficiencies of the technique by Quimby and Yen [9]. For the first time, we demonstrate suitability of infrared photothermal radiometry (PTR) [13] to the determination of η_R and τ in a laser material (ruby). The ability of PTR to access high frequencies (>100 kHz) renders it a viable candidate for the study of other laser materials with short metastable level lifetimes. We further developed a simple analytical technique based on extrema in the PTR phase and amplitude slope, to obtain unambiguous η_R and τ information for both amplitude and phase of the signal. These quantities may be determined self-consistently and uniquely from a single frequency scan at one (arbitrary) excitation laser line, provided the photon energy can populate the metastable level.

II. PTR of Three-Level Laser Materials

Tom *et al.* [14] have presented a generalized model of the photothermal radiometric response to optical excitation of non-opaque matter. Under the 1-D laser beam geometry assumption, they derived a complicated analytical expression relating the PTR signal in the frequency domain to the optical and thermal properties of the sample. These authors further assumed no excited-state dynamic behavior, in that the solid system under consideration de-excites "instantaneously" with respect to the period of the sinusoidal modulation of the incident light intensity. They showed that radiative heat emission following heat absorption (Kirchoff's law) is not important in PTR applications for the determination of the temperature oscillation, and may be neglected. This reduces the nonlinear integrodifferential heat diffusion (thermal-wave) equation containing the heat source due to absorption of thermal radiation to a simpler linear differential equation for diffusion. A further simplification occurs in linearizing the temperature dependence of the diffusion equation due to convective heat flux from a 5/4-power, and showing that normally the convective heat flux is small compared to the conductive flux.

Under these conditions, the dependence of the PTR signal on parameters of interest to this paper involves: i) the absorption coefficient $\beta(\lambda)$ at the visible exciting optical wavelength λ; and ii) the mean infrared absorption coefficient β_o an averaged value over the spectrum of the black-body thermal-wave radiation emitted as a result of optical absorption of the incident radiation and subsequent heat release in the material following nonradiative de-excitation:

$$\beta_o = \overline{\beta(\lambda_{ir})}. \tag{1}$$

Equation (1) corresponds to the "gray body" approximation of radiative heat transfer. Experimentally, the range of λ_{ir} depends on the spectral bandwidth of the IR detector employed.

For the test case of a ruby crystal, the value of β_o is very large in the 8–12 μm detection spectral window of our HgCdTe sensor. Using the transmission of a CO_2 laser beam, it was estimated that $\beta_o > 10^4$ cm^{-1}, so that $\beta_o l \gg 1$, where l is the thickness of the laser rod: $l = 6$ cm. From the calculated absorption spectrum of the ruby crystal following optical transmission measurements, Fig. 1, it was found that β (514.5 nm) = 0.325 cm^{-1} at the 514.5 nm line of the Ar^+ laser. Using the value of thermal diffusivity $\alpha = 0.13$ cm^2/s [15] in the expression for the ruby thermal diffusion length [16]

$$\mu(f) = (\alpha/\pi f)^{1/2} \tag{2}$$

the range of μ values covered in the experimental frequency scan (5–200 Hz) was found to be 9.10×10^{-2} cm $\geq \mu(f) \geq 1.4 \times 10^{-2}$ cm. It was thus verified that in the entire range of experimental interest, $\beta(514.5\text{ nm})\,\mu(f) \ll 1$. The conditions

$$\beta_o l \gg 1, \quad \beta\mu \ll 1 \tag{3}$$

correspond to the following simplified form of the complex PTR signal expression by Tom *et al.* (Case 2(a) of [14]):

$$W_{ac}(\omega, t) = 4\alpha Q[A(t)/\omega]e^{-i\pi/2} \tag{4}$$

where

$$Q = \epsilon\bar{\sigma}T_o^3/k \tag{5a}$$

a constant in a given experiment, and

$$A(t) = \tfrac{1}{2} I_o \beta e^{i\omega t}. \tag{5b}$$

Here ϵ is the effective emissivity of the sample; $\bar{\sigma} = n^2\sigma$ where n is the IR index of refraction of the sample and σ is the Stefan–Boltzmann constant; T_o is the ambient temperature; I_o is the incident laser intensity; and k is the sample thermal conductivity.

Equation (4) is valid for "instantaneously" de-exciting materials. For a solid-state laser medium exhibiting three-level behavior, such as the $Cr^{3+}:Al_2O_3$ system, Fig. 2, this equation must be modified. Assuming a modulated pumping rate to level $|3\rangle$ given by

$$W_p(\omega, t) = \tfrac{1}{2} W_{po}(1 + e^{i\omega t}) \tag{6}$$

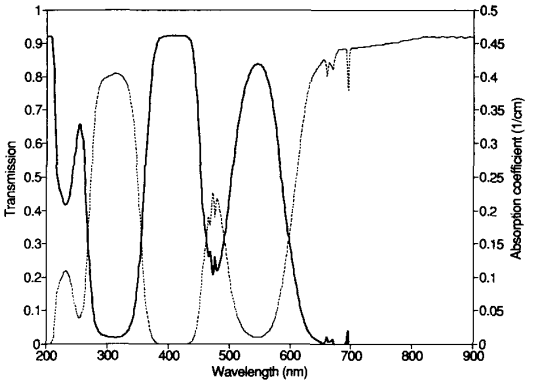

Fig. 1. The optical spectrum of the test ruby crystal obtained with light incident normal to the polished surface of the crystal. (———) Absorption coefficient; (-----) optical transmission. The coefficient of absorption was calculated from the transmitted intensity, I_T and $\beta = (1/l) \ln [1 - r/I_T + r(1 - r)]$ where $r = [(n - 1)/(n + 1)]^2$ at normal incidence (n: index of refraction, calculated from the reflectivity curve of the sample).

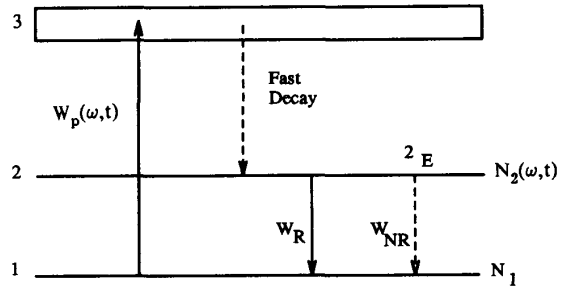

Fig. 2. Simplified electronic energy kinetics diagram for a three-level system, such as ruby ($Cr^{3+}:Al_2O_3$).

the optical pumping by the excitation laser beam photons will drive a synchronous modulated population of the metastable level $|2\rangle$

$$N_2(\omega, t) = \tfrac{1}{2} N_2^{(o)}(\omega)(1 + e^{i\omega t}). \tag{7}$$

It can be further assumed that N_1 is constant [9], valid for sufficiently weak pumping of the ground state $|1\rangle$, which is, nevertheless, always heavily populated. Neglecting the initial condition term in the rate equation of level $|2\rangle$, which accounts for the presence of residual (or cavity) photons before the onset of each half cycle of laser beam irradiation [17]

$$\frac{d}{dt} N_2(\omega, t) = N_1 W_p(\omega, t) - \frac{N_2(\omega, t)}{\tau_{21}} \tag{8}$$

where

$$\tau_{21} = \frac{1}{W_R + W_{NR}}. \tag{9}$$

As the result of the slow $|2\rangle \rightarrow |1\rangle$ decay, preceded by the fast nonradiative $|3\rangle \rightarrow |2\rangle$ transition, the thermal power density [J/cm^{3}s] which is released in the laser material is

$$A(\omega, t) = \tfrac{1}{2} [N_1 W_{po} E_{32} + (\eta_{NR}/\tau_{21}) N_2^{(o)}(\omega) E_{21}](1 + e^{i\omega t}) \tag{10}$$

where

$$\eta_{NR} = 1 - \eta_R = \frac{\tau_{21}}{\tau_{NR}} = \frac{W_{NR}}{W_R + W_{NR}}. \tag{11}$$

From the solution of (8) subject to (6), (7) we obtain

$$N_2^{(o)}(\omega) = N_1 \left(\frac{W_{po} \tau_{21}}{1 + i\omega\tau_{21}} \right). \tag{12}$$

Furthermore, the absorption coefficient β_{31}, at the excitation wavelength is proportional to the population of level $|1\rangle$:

$$\beta_{31} I_o = N_1 W_{po} E_{31}. \tag{13}$$

Substituting from (12) and (13) into (10), the ac component of the released thermal power density becomes $A(\omega, t)$ replacing the constant A in (4):

$$A(\omega, t) = \frac{1}{2} I_o \beta_{31} \left(\frac{E_{32}}{E_{31}} \right) \left[1 + \left(\frac{E_{21}}{E_{32}} \right) \frac{\eta_{NR}}{1 + i\omega\tau_{21}} \right] e^{i\omega t}. \tag{14}$$

In the case of fast ($\omega\tau_{21}, << 1$), entirely nonradiative ($W_R = 0 \Rightarrow \eta_{NR} = 1$) decay, (14) reduces to

$$A(\omega, t) = \tfrac{1}{2} I_o \beta_{31} e^{i\omega t}. \tag{14a}$$

This is the limit in which the PTR (4) has been derived [14]. It is clear from this analysis that (14) must now be modified as follows:

$$W_{ac}(\omega) = \frac{2\epsilon\bar{\sigma} T_o^3}{k\omega} I_o \beta_{31} F(\omega) e^{-i\pi/2} \tag{15}$$

where the temporal modulation factor $e^{i\omega t}$ was suppressed for simplicity. The function $F(\omega)$ contains the dynamic/kinetic information of the three-level system. In terms of PTR signal amplitude and phase

$$F(\omega) = |F(\omega)| e^{-i\phi(\omega)} \tag{16}$$

where

$$|F(\omega)| = (E_{32}/E_{21}) \left\{ \left[1 + \frac{\eta_{NR}(E_{21}/E_{32})}{1 + (\omega\tau_{21})^2} \right]^2 + \left[\frac{\eta_{NR}\omega\tau_{21}(E_{21}/E_{32})}{1 + (\omega\tau_{21})^2} \right]^2 \right\}^{1/2} \tag{17a}$$

and

$$\phi(\omega) = \tan^{-1} \left[\frac{\eta_{NR}\omega\tau_{21}(E_{21}/E_{32})}{1 + (\omega\tau_{21})^2 + \eta_{NR}(E_{21}/E_{32})} \right]. \tag{17b}$$

III. Experimental and Discussion

Experiments were performed to obtain both the photothermal (PTR) and luminescence frequency response of a cylindrical ruby sample, 6 cm in length and 1 cm in

diameter [18]. The two flat surfaces were polished smooth, whereas the curved surface was rough and light scattering. Fig. 3 shows the dual experimental setup: A CW Innova 100 Ar^+ laser from Coherent was used as a pump with output power ≤ 2.5 W at 514.5 nm. The blackbody radiation from the optically excited ruby crystal surface was collected and collimated by two Ag-coated off-axis paraboloidal mirrors, and subsequently focused on the active area of a HgCdTe detector (EG & G Judson Model J15D12)/pre-amplifier element with frequency bandwidth between dc and 1 MHz. The detector was fitted with a GE window which filtered out the excitation beam. The spectral response bandwidth of the detector was in the 8–12 μm range. The PTR signal from the preamplifier (EG&G Judson Model PA-350) was fed into an EG&G Model 5210 lock-in analyzer. The internal reference square-wave voltage generator of the lock-in was used to drive the AOM and to automatically change the modulation frequency applied to it. This setup therefore allowed computer-controlled automated frequency scans of the modulated laser intensity. Luminescence emitted through the curved side surface of the optically pumped ruby rod was filtered from excitation line photons using a sharp cut-off glass filter (Melles-Griot Model 0G550) acting as a low-pass filter in front of a fast(ns) risetime Si photodiode. The photovoltage generated by the spectrally integrated luminescence of our crystal, the spectrum of which is shown in Fig. 4, was fed into an EG&G Model 5210 lock-in analyzer and the amplitudes and phases of both PTR and luminescence signals were stored in the computer. In order to account for the instrumental transfer function, it was found convenient to pump the rough side of the ruby rod and use the PTR signal thus generated to normalize the frequency response of the flat polished surface. It was observed that negligible luminescence was generated when the laser beam was incident on the side, and that the laser beam was absorbed much more strongly here. Under optically opaque conditions the predicted PTR dependence is given by Tom *et al.* (Case 1 of [14]):

$$W_{ac}(\omega, t) = (2A\alpha^{1/2}/\omega^{1/2})e^{-i\pi/4}. \quad (18)$$

It was, indeed, found that the signal phase from the pumped side surface was leading the phase from the flat surface by $\pi/4$, in agreement with (4) and (18). The amplitude ratio for materials exhibiting instantaneous relaxation is expected to be

$$|W_{ac}(\omega)|_{\substack{\text{transparent}\\\text{opaque}\\\text{reference}}}/W_{ac}(\omega)|_{\substack{\text{transparent}\\\text{opaque}\\\text{reference}}} = \text{const.} \times \omega^{-1/2}. \quad (19)$$

These signal normalization considerations are also important for solid-state laser materials studies and are very easy to implement: the instrumental frequency response from an opaque surface, such as the rough side of the ruby rod, with no delay relaxation, as witnessed by the lack of luminescence after pumping that side, is very reproducible and can be stored in the computer memory once, to be used with all subsequent sample data. Rationing amplitudes and subtracting phases in each frequency scan normalizes out the instrumental transfer function.

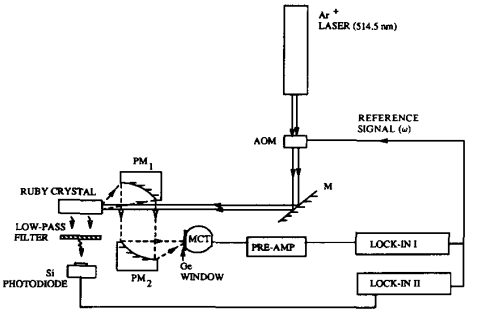

Fig. 3. Experimental setup for PTR and luminescence measurements. AOM: Acoustooptic modulator; M: mirror; PM_1, PM_2: off-axis parabolic mirrors: MCT: HgCdTe detector, EG&G Judson Model J15-D12, dc-coupled with fitted Ge window.

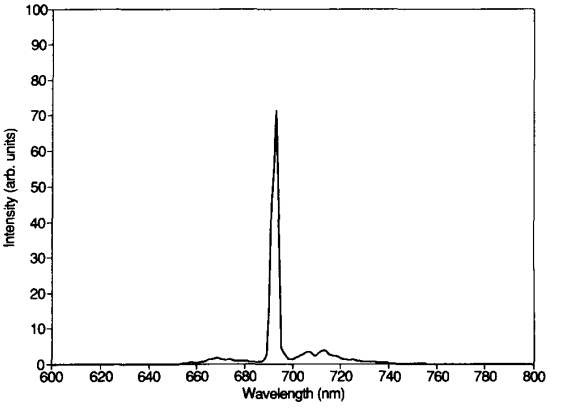

Fig. 4. Ruby crystal luminescence spectrum. Note the strong domination of the ^2E metastable state luminescence at 694.5 nm.

Fig. 5 shows the PTR phase and amplitude slope dependence on modulation frequency. Fig. 5a shows a polynomial fit to the experimental amplitude slope. The minimum of the fitting curve is at 36 Hz. The ordinate in Fig. 5(a) was obtained, in view of (19), by numerically differentiating the quantity

$$(|W_{ac}(f_j)|_{\text{polished}}/|W_{ac}(f_j)|_{\text{rough}}) \times \sqrt{f_j}.$$

Assuming that $\eta_{NR} << 1$ for ruby [9], the only ω dependence of the above quantity should be that of $|F(\omega)|$, (17a), which can thus be approximated

$$|F(\omega)|_{\eta_{NR}<<1} \simeq (E_{32}/E_{21})\left[1 + \frac{\eta_{NR}(E_{21}/E_{32})}{1 + (\omega\tau_{21})^2}\right]. \quad (20)$$

This function of ω predicts a slope with a minimum at a frequency f_A^{PTR}, such that

$$\tau_{21} = \frac{1}{2\sqrt{3}\,\pi f_A^{\text{PTR}}}. \quad (21)$$

The experimental data with the (average value) polynomial fit with $f_A^{\text{PTR}} = 36$ Hz $\pm$ 9 Hz yield the range of values

$$2.14 \text{ ms} \leq \tau_{21} \leq 3.5 \text{ ms} \quad (22)$$

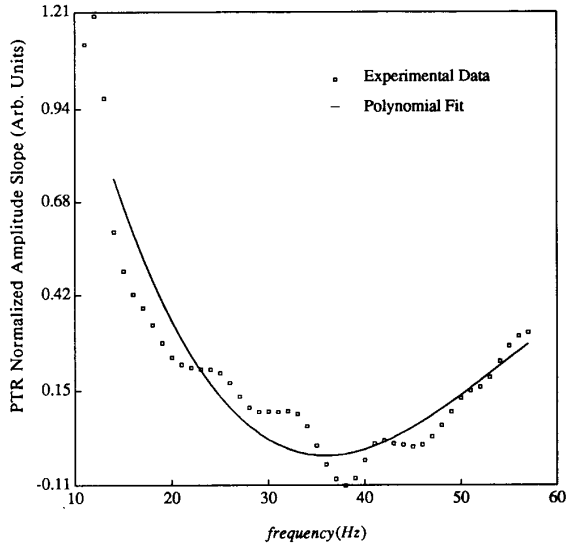

(a)

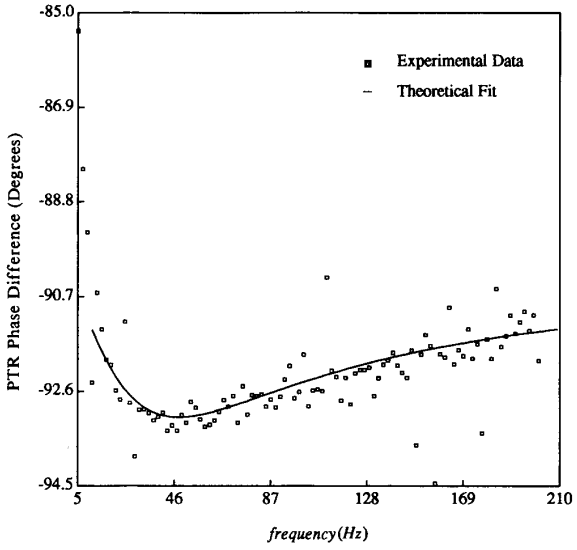

(b)

Fig. 5. Normalized PTR signal data from ruby crystal: (a) Amplitude slope. Continuous line: best polynomial fit with $f_A^{\mathrm{PTR}} = 36$ Hz; (b) Phase. Continuous line: best fit to (17b) with $f_p^{\mathrm{PTR}} = 45$ Hz.

in agreement with the earlier reported PAS value of 2.7 ms [9]. The noise in all presented data curves in this work was of a magnitude such that:

$$\mathrm{SNR} = \frac{\text{Mean Value}}{\text{Standard Deviation}} \geq 60.$$

Fig. 6 shows the respective luminescence data. The rate equation (8) leads to the population modulation (12), which is responsible for radiative emission from the level ^2E in ruby. Therefore, the luminescence signal

$$S(\omega) = \text{const.} \times N_2^{(o)}(\omega) = \text{const.} \times |N_2^{(o)}| e^{-i\theta_2} \tag{23a}$$

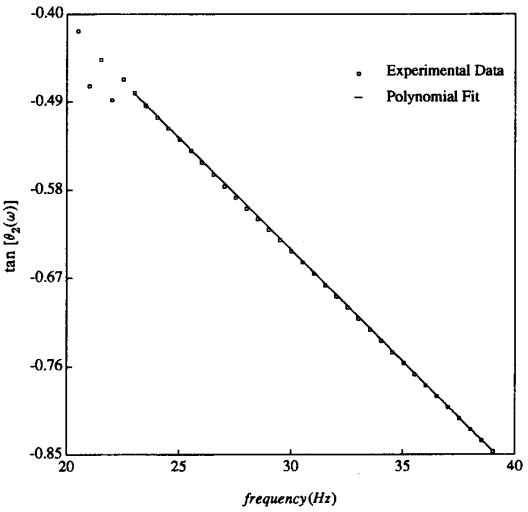

(a)

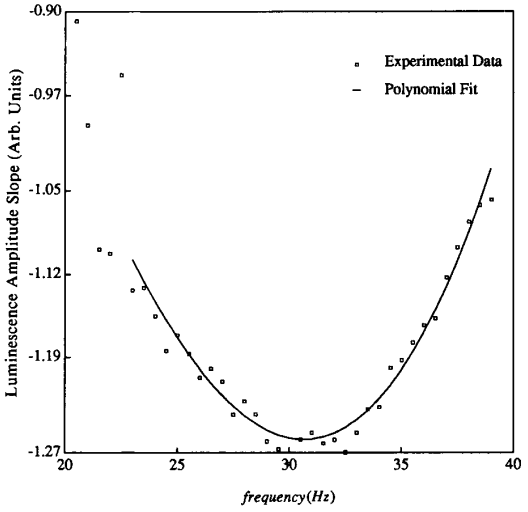

(b)

Fig. 6. Luminescence signal data from ruby crystal; (a) Phase. Continuous line: best fit to (23c); (b) Amplitude slope. Continuous line: best polynomial fit with $f_A^{\mathrm{LUM}} = 30$ Hz.

with

$$|N_2^{(o)}(\omega)| = \frac{N_1 W_{po} \tau_{21}}{\sqrt{1 + (\omega\tau_{21})^2}} \tag{23b}$$

and

$$\theta_2(\omega) = \tan^{-1}(\omega\tau_{21}). \tag{23c}$$

Fig. 6(a) exhibits the expected linear behavior of tan θ_2 versus ω, with some deviation below 22 Hz. From the slope of that curve we obtained

$$\tau_{21} = 3.63 \text{ ms} \tag{24}$$

at the high end of the values calculated from the PTR amplitude slope, yet in good agreement with earlier optically

obtained values [15]. Subsequent experiments with pulsed laser excitation and PMT detection exhibited exponentially decaying luminescence from which the value $\tau_{21} = 3.78$ ms was extracted, in good agreement with (24). The generally superior SNR of the luminescence signal, compared to the lower dynamic range of the PTR signal (a feature shared with other photothermal techniques), renders the value $\tau_{21} \approx 3.63$ ms more reliable than the mean value 2.55 ms calculated from Fig. 5(a). In addition, the luminescence amplitude also carries τ_{21} information. As a function of ω, (23a) predicts a slope with a minimum at a frequency f_A^{LUM}, such that

$$\tau_{21} = \frac{1}{2\sqrt{2}\,\pi f_A^{\mathrm{LUM}}}. \tag{25}$$

From the data in Fig. 6(b) one obtains

$$3.52 \text{ ms} \leq \tau_{21} \leq 3.88 \text{ ms} \tag{26}$$

consistent with the luminescence phase data. Using pulsed laser excitation of the ruby rod at 475 nm in a separate measurement we obtained a purely exponential luminescence decay signal, in agreement with the transient solution to the rate equation (8), which gives:

$$N_2(t) = \text{const.} \times e^{-t/\tau_{21}}. \tag{27}$$

The time constant measured at 694 nm was

$$\tau_{21} = 3.786 \pm 0.005 \text{ ms} \tag{28}$$

well within the range of the values (26). Now using the value $\tau_{21} = 3.63$ ms obtained from the slope of Fig. 6(a) in the PTR phase expression $\phi(\omega)$, (17b), with η_{NR} as the only adjustable parameter, the best-fitted theoretical curve in Fig. 5(b) was drawn. For this fit the following values were used:

$$E_{21} = 1.79 \text{ eV},$$

$$E_{32} = E_{31} - E_{21} = 2.4 \text{ eV} - 1.79 \text{ eV} = 0.62 \text{ eV}.$$

Therefore, $(E_{21}/E_{32}) = 2.88$ for 514.5 nm photons. The best fit produced the value $\eta_{NR} = 0.04$, or

$$\eta_R = 0.96.$$

It can be easily verified that (17b) exhibits a minimum at a frequency f_p^{PTR}, such that

$$\eta_{NR} = 1 - \eta_R = (E_{32}/E_{21})[(2\pi\tau_{21} f_p^{\mathrm{PTR}})^2 - 1]. \tag{29}$$

The best fit of Fig. 5(b) shows some deviation below approximately 20 Hz, in agreement with the luminescence phase deviation frequency range, Fig. 6(a). The value $\eta_R = 0.96$ appears to be very reliable as a result of the excellent fit of the theory to the data in Fig. 5(b). From the range (26) of τ_{21} obtained through the minimum in the luminescence amplitude slope, the following range of η_R results when use is made of the experimental PTR phase minimum $f_p^{\mathrm{PTR}} = 46$ Hz, and of (29):

$$0.90 < \eta_R < 0.98. \tag{30}$$

These values are consistent with the conclusions of Quimby and Yen [9] and earlier references named therein.

IV. Conclusion

Self-consistent PTR and luminescence frequency-scanned measurements of a ruby laser rod were performed. The data were analyzed in terms of photothermal and optical models, respectively, of a conventional three-level solid-state laser medium. Expressions were found for the extrema in the frequency response curves of the PTR amplitude slope and phase, as well as for the extremum in the luminescence amplitude slope. The τ_{21} dependence of the PTR amplitude slope minimum and the (τ_{21}, η_{NR}) dependence of the phase minimum can be used self-consistently to yield a unique pair of (τ_{21}, η_{NR}) values for a given laser material. In practice, it seems that the optimal combination of measurements in terms of SNR for these parameters involves the luminescence phase slope (τ_{21}) and the PTR phase minimum $(\eta_{NR} \rightarrow \eta_R)$. The broad frequency response of frequency-domain PTR is, in principle, capable of extending these measurements to solid-state lasers with sub-millisecond lifetimes and work is in progress on the $Ti^{3+}:Al_2O_3$ system.

The present work has demonstrated that (τ, η_R) measurements can be simply and accurately performed in a single-ended manner, with no need for precise and complicated dual wavelength operation, or photoacoustic gas-cell geometry restrictions as is the case with Quimby and Yen's method [9].

References

[1] L. D. Merkle and R. C. Powell, "Photoacoustic spectroscopy investigation of radiationless transitions in Eu^{2+} ions in KCl crystal," *Chem. Phys. Lett.*, vol. 46, pp. 303-306, 1977.

[2] A. Rosencwaig and E. A. Hildum, "Nd^{3+} fluorescence quantum-efficiency measurements with photoacoustics," *Phys. Rev. B.*, vol. 23, pp. 3301-3307, 1981.

[3] R. S. Quimby and W. M. Yen, "Photoacoustic measurement of absolute quantum efficiencies in solids," *Opt. Lett.*, vol. 3, pp. 181-183, 1978.

[4] J. C. Murphy and L. C. Aamodt, "Photoacoustic spectroscopy of luminescent solids: Ruby," *J. Appl. Phys.*, vol. 48, pp. 3502-3509, 1977.

[5] J. Hamilton, I. Duncan, and T. Morrow, "Anomalous wavelength-dependent effects in photoacoustic measurements of Nd^{3+} luminescence quantum efficiency in various laser materials," *J. Lumin.*, vol. 33, pp. 1-33, 1985.

[6] A. Mandelis, "Photoacoustic determination of the non-radiative quantum efficiency of uranyl formate monohydrate, $UO^2(HCOO)^2 \cdot H_2O$, powders," *Chem. Phys. Lett.*, vol. 91, pp. 501-505, 1982.

[7] W. Lahmann and H. J. Ludewig, "Opto-acoustic determination of absolute quantum yields in fluorescent solution," *Chem. Phys. Lett.*, vol. 45, pp. 177-179, 1977.

[8] R. C. Powell, D. P. Neikirk, J. M. Flaherty, and J. G. Gualtieri, "Lifetime measurements, infrared and photoacoustic spectroscopy of NdP_5O_{14}," *J. Phys. Chem. Solids*, vol. 41, pp. 345-350, 1980.

[9] R. S. Quimby and W. M. Yen, "Photoacoustic measurement of the ruby quantum efficiency," *J. Appl. Phys.*, vol. 51, pp. 1780-1782, 1980.

[10] M. L. Shand, "Quantum efficiency of alexandrite," *J. Appl. Phys*, vol. 54, pp. 2602-2604, 1983.

[11] A. Mandelis and B. S. H. Royce, "Relaxation time measurements in frequency and time-domain photoacoustic spectroscopy of condensed phases," *J. Opt. Soc. Amer.*, vol. 70, pp. 474-480, 1980.

[12] P. Albers, E. Stark, and G. Huber, "Continuous-wave laser opera-

tion and quantum efficiency of titanium-doped sapphire," *J. Opt. Soc. Amer. B.*, vol. 3, pp. 134-139, 1986.
[13] A. C. Tam, in *Photoacoustic and Thermal-Wave Phenomena in Semiconductors*, A. Mandelis, Ed. New York: North-Holland, 1987, pp. 176-197.
[14] R. D. Tom, E. P. O'Hara, and D. Benin, "A generalized model of photothermal radiometry," *J. Appl. Phys.*, vol. 53, pp. 5392-5400, 1982.
[15] W. Koechner, *Solid State Laser Engineering*, Springer Ser. Opt. Sci., vol. 1, ch. 2.2, pp. 44-53.
[16] A. Rosencwaig and A. Gersho, "Theory of the photoacoustic effect with solids," *J. Appl. Phys.*, vol. 47, pp. 64-69, 1976.
[17] B. di Bartolo in *spectroscopy of Solid-State Laser-Type Materials*, B. di Bartolo, Ed. New York: Plenum, 1987, pp. 31-108.
[18] Courtesy Boris Stoicheff, Dept. of Physics, University of Toronto.

Andreas Mandelis, photograph and biography not available at the time of publication.

Mahendra Munidasa, photograph and biography not available at the time of publication.

Andreas Othonos, photograph and biography not available at the time of publication.